Structural Engineering and Mechanics, *Vol. 52, No. 5 (2014) 997-1017*
DOI: http://dx.doi.org/10.12989/sem.2014.52.5.997

The modal characteristics of non-uniform multi-span continuous beam bridges

Lu-ning Shi[a], Wei-ming Yan[*1] and Hao-xiang He[b]

Beijing Laboratory of Earthquake Engineering and Structure Retrofit, Beijing University of Technology, Beijing 100124, China

(Received May 26, 2014, Revised July 19, 2014, Accepted August 20, 2014)

Abstract. According to the structure characteristics of the non-uniform beam bridge, a practical model for calculating the vibration equation of the non-uniform beam bridge is given and the application scope of the model includes not only the beam bridge structure but also the non-uniform beam with added masses and elastic supports. Based on the Bernoulli-Euler beam theory, extending the application of the modal perturbation method and establishment of a semi-analytical method for solving the vibration equation of the non-uniform beam with added masses and elastic supports based is able to be made. In the modal subspace of the uniform beam with the elastic supports, the variable coefficient differential equation that describes the dynamic behavior of the non-uniform beam is converted to nonlinear algebraic equations. Extending the application of the modal perturbation method is suitable for solving the vibration equation of the simply supported and continuous non-uniform beam with its arbitrary added masses and elastic supports. The examples, that are analyzed, demonstrate the high precision and fast convergence speed of the method. Further study of the timesaving method for the dynamic characteristics of symmetrical beam and the symmetry of mode shape should be developed. Eventually, the effects of elastic supports and added masses on dynamic characteristics of the three-span non-uniform beam bridge are reported.

Keywords: modal perturbation method; analytic solution; non-uniform beam; elastic support; added mass; mode shape

1. Introduction

Non-uniform beams are widely used in the building of highway bridges, railroad bridges and city bridges. The theory and experimental research on the dynamic characteristics of the non-uniform beam is becoming more and more popular. However, the vibration equation of the non-uniform beam has complex forms of variable coefficient differential equation and only some special structures can obtain the analytical solution (Chen and Wu 2002, Kamke 1980) of the vibration equation. For the non-uniform beam bridge, the vibration equation is too complicated to obtain the exact solution because of the changing discontinuity of the support cross-section, the

∗Corresponding author, Ph.D., E-mail: yanwm@bjut.edu.cn
[a]Ph.D. Student, E-mail: shiluning1987@163.com
[b]Ph.D., E-mail: hhx7856@emails.bjut.edu.cn

http://www.techno-press.org/?journal=sem&subpage=8 ISSN: 1225-4568 (Print), 1598-6217 (Online)

hinged edge, which is not ideal and the weight of the diaphragm. The calculation of the vibration equation of the non-uniform beam bridge normally used is the simplified model, because the supports are simplified as hinge bearing and the weight of diaphragm is ignored, which may result in calculation error. This error in the long-span non-uniform beam bridge can't be ignored (Pratiher 2012, Bambill *et al*. 2013). It is necessary to make reasonable assumptions and simplifications according to the structure characteristics of the non-uniform beam bridge and refine a practical model for calculating the vibration equation of non-uniform beam with arbitrary added masses and elastic supports. At the same time, to find an appropriate method to solve the vibration equation of the non-uniform beam according to the computational model and obtain the more accurate solutions. In recent years, international scholars have done a lot of research on the dynamic characteristics of the non-uniform beam and have obtained some results.

Bahrami *et al*. (2011) used the wave propagation method to study the vibration of the beams with variable cross-sections. The beam is partitioned into several continuous segments, each with a uniform cross-section, for which there exists an exact analytical solution. Firouz-Abadi *et al*. (2007) employed the WKB approximation to investigate the transverse free vibration of a class of variable-cross-section beams and obtained a singular differential equation in terms of the natural frequency of vibration. Sarkar and Ganguli (2013) studied the free vibration of a non-uniform free–free Euler–Bernoulli beam using an inverse problem approach. Qian and Yue (2011) presented the numerical calculation method for the natural frequency of the transverse vibration of the simply supported none-uniform beam by using the finite difference method. Utilizing the Hilbert space methods, Jovanovic (2011) derived the generalized Fourier series solution for the transverse vibration of a beam that was subjected to a viscous boundary and numerical simulations. The above research was unable to take into account, effectively, the influence of elastic supports and added masses. Mao (2011), Hsu *et al.* (2008) studied the free vibration problems of the non-uniform Euler-Bernoulli beam under various supporting conditions based on the Adomian decomposition method (ADM). Ho and Chen (1998) introduced using the differential transformation method to solve the free and forced vibration problems of a general elastically end restrained non-uniform beam. Huang and Li (2010) studied the free vibration of axially functional graded beams with a non-uniform cross-section and natural frequencies. The above studies didn't consider the influence of added mass for the dynamic characteristics of the beam. Elishakoff and Johnson (2005) focused on the free vibration of the uniform or non-uniform cross-section beams that carry the concentrated masses and utilized the semi-inverse method on the closed-form solution. This method, however, was not suitable for the beam with elastic supports. DeRosa *et al*. (1996), Xia *et al*. (2000) presented an accurate analytical method for natural vibrations of the beams with lumped masses and elastic supports, which only applied to the uniform beam. Lou *et al.* (2005), Pan *et al*. (2012) introduced the mode perturbation method (MPM) to analyze the dynamic characteristics of Timoshenko beams. In this approach, the differential equation of motion, describing the dynamic behavior of the Timoshenko beam, can be transformed into a set of nonlinear algebraic equations. In the bridge and mechanical structures, using the MPM (Lou *et al.* 2005, Pan *et al*. 2012, Lou and Wu 1997) directly to solve the modal parameters of the non-uniform beam is unable to take the support stiffness and the added mass on the supports into consideration, which can also have an effect on the dynamic characteristics of the structure. In this paper, a practical model for calculating the vibration equation of the non-uniform Bernoulli-Euler beam with arbitrary added masses and elastic supports is given. The application of the modal perturbation method is extended to solve the dynamic characteristics of the calculation model. Practical examples are presented to show the increase accuracy of the extending the application of

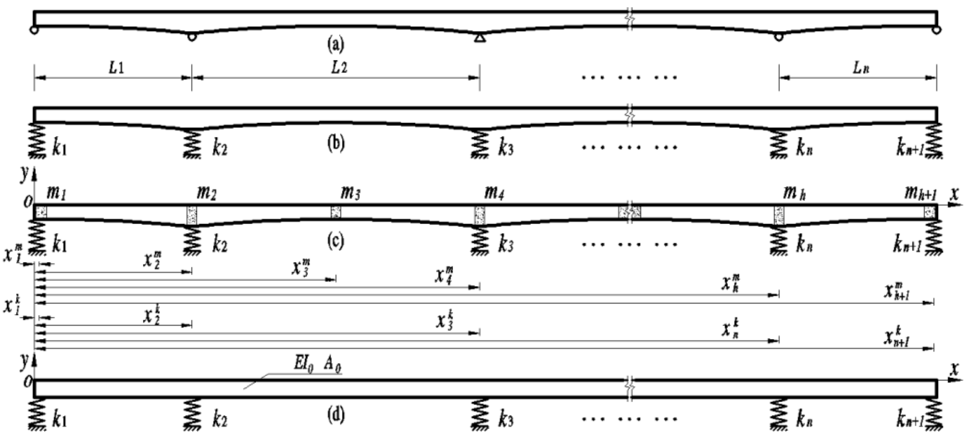

Fig. 1 Calculation model of non-uniform beam

the modal perturbation method. Furthermore, simplify calculating method for symmetrical beam has been studied based on the symmetry of mode shape. Eventually, the effects of elastic supports and added masses on dynamic characteristics of the three-span non-uniform beam bridge are reported.

2. The calculation model

The dynamic characteristics of the non-uniform beam is affected by support stiffness and added mass. The support ensured the free deformation of the beam under such factors as load, temperature change and concrete shrinkage, which must have enough vertical stiffness and elasticity. The beam must have enough lateral stiffness to prevent the cross-section from deformation of distortion, bending-torsion and warping, which is usually set on the diaphragm of the individual section of the beam. In general, it is thought that the greater the stiffness of the diaphragm, the better the beam’s integrity. So the diaphragm is generally thicker (Yang *et al*. 2010) and the diaphragm of the concrete beam will produce a larger added mass. However, the Eigenvalue analysis of beams usually ignores the influence of the actual support stiffness and added mass produced by the diaphragm and other factors (Lee and Yhim 2005, Bedon and Morassi 2014). The calculation model, which does take into account the influence of the actual support stiffness and added mass, is shown in Fig. 1(a). The calculation model, which only considers the influence of the actual support stiffness, is shown in Fig. 1(b). The consideration of the influence of the actual support stiffness and added mass to the dynamic characteristics of non-uniform beam, the mechanical calculation model of the dynamic characteristics of non-uniform beam with arbitrary added masses and elastic supports provides more accuracy, as shown in Fig. 1(c). The model considers the actual support stiffness and added mass influence on the dynamic characteristics of non-uniform beam effectively.

3. Vibration equation of non-uniform beam with arbitrary added masses and elastic supports

The free vibration equation of non-uniform Bernoulli-Euler beam with h+1 added masses m_a (a=1, 2,$\cdots$, h+1) and n+1 elastic supports k_b (b=1, 2, $\cdots$, n+1), as shown in Fig. 1(c), can be written as (Ho and Chen 1998, Xia *et al*. 2000)

$$\frac{\partial^2}{\partial x^2}\left[EI(x)\frac{\partial^2\mu(x,t)}{\partial x^2}\right]+\rho A(x)\frac{\partial^2\mu(x,t)}{\partial t^2}+\sum_{a=1}^{h+1}m_a\delta\left(x-x_a^m\right)\frac{\partial^2\mu(x,t)}{\partial t^2}+\sum_{b=1}^{n+1}k_b\delta\left(x-x_b^s\right)\mu(x,t)=0 \quad (1)$$

where x is axial coordinate, $\mu(x,t)$ is the transverse deflection, E is Young's modulus, ρ is the mass density of the beam material, $A(x)$ is the cross-sectional area of the non-uniform beam at the position x, $I(x)$ is the moment of inertia of $A(x)$, t is the time, δ is Dirac function, x_a^m is the axial coordinate of the added mass m_a and x_b^s is the axial coordinate of the elastic support k_b .

For any mode of vibration, the lateral deflection $\mu(x,t)$ may be written in the form (Clough and Penzien 2003, Timoshenko 1974)

$$\mu(x,t)=\bar{\phi}(x)q(t) \quad (2)$$

where $\bar{\phi}(x)$ is the modal deflection and $q(t)$ is a harmonic function of time t. then substitution of Eq. (2) into Eq. (1) yields

$$\frac{\partial^2}{\partial x^2}\left[EI(x)\frac{\partial^2\bar{\phi}(x)}{\partial x^2}\right]-\bar{\lambda}\rho A(x)\bar{\phi}(x)-\bar{\lambda}\sum_{a=1}^{h+1}m_a\delta\left(x-x_a^m\right)\bar{\phi}(x)+\sum_{b=1}^{n+1}k_b\delta\left(x-x_b^s\right)\bar{\phi}(x)=0 \quad (3)$$

where $\bar{\lambda}=\bar{\varpi}^2$ is the eigenvalue of the non-uniform Bernoulli-Euler beam and $\bar{\varpi}$ is the angular frequency. Eq. (3) is a high-order variable coefficient differential equation which is more difficult to obtain the analytical solution and is typically solved by the approximate method. This paper extended the application of the modal perturbation method (Lou *et al*. 2005, Pan *et al*. 2012) to solve the vibration problem of the non-uniform Euler-Bernoulli beam with arbitrary added masses and elastic supports and achieve an accurate and efficient semi-analytical method for solving Eq. (3).

4. The principle of MPM

4.1 Mathematical formulation.

The uniform Bernoulli- Euler beam with elastic supports, which is shown in Fig. 1(d) has the same span length, material characteristics and boundary conditions as the non-uniform beam. The moment of inertia and area of the uniform beam are calculated to be the average value of the non-uniform beam as follows

$$I_0=\frac{1}{L}\int_0^L I(x)dx \quad (4)$$

$$A_0=\frac{1}{L}\int_0^L A(x)dx \quad (5)$$

where A_0 is the cross-sectional area of the uniform beam, I_0 is the moment of inertia of A_0 and L is the sum of span length of uniform beam, as shown in Fig. 1.

The moment of inertia and area of the non-uniform beam can be written as

$$I(x) = I_0 + \Delta I(x) \tag{6}$$

$$A(x) = A_0 + \Delta A(x) \tag{7}$$

where $A(x)$ is the cross-sectional area of the non-uniform beam, $I(x)$ is the moment of inertia of $A(x)$, $\Delta A(x)$ is the increment of the cross-sectional area, $\Delta I(x)$ is the increment of inertia moment of $\Delta A(x)$. The free vibration equation of the uniform beam with complete elastic supports is obtained

$$EI_0 \frac{\partial^4 \mu(x,t)}{\partial x^4} + \rho A_0 \frac{\partial^2 \mu(x,t)}{\partial t^2} + \sum_{b=1}^{n+1} k_b \delta(x - x_b^s) \mu(x,t) = 0 \tag{8}$$

Obviously, Eq. (8) is different with the modal perturbation method (Lou *et al*. 2005, Pan *et al*. 2012). Assumption that λ_i and $\phi_i(x)$ is the i^{th} eigenvalue and eigen function of the uniform Bernoulli-Euler beam, respectively. The Eq. (8) can be expressed into

$$EI_0 \phi_i^4(x) - \lambda_i \rho A_0 \phi_i(x) + \sum_{b=1}^{n+1} k_b \delta(x - x_b^s) \phi_i(x) = 0 \tag{9}$$

The modal solution of Eq. (9) is shown in Appendix C. To obtain the eigenvalues and eigen functions of the non-uniform Bernoulli-Euler beam with added masses and elastic supports described in Eq. (3), this paper extended the application of the modal perturbation method in solving the process of the vibration equation. The variable coefficient differential equation, which describes the dynamic behavior of the non-uniform Bernoulli-Euler beam, is converted to nonlinear algebraic equations. The eigenvalues and eigen functions of the non-uniform Bernoulli-Euler beam can actually solve the nonlinear algebraic equations. The i^{th} eigenvalue and eigen function of the non-uniform Bernoulli-Euler beam with added masses and elastic supports is written as

$$\bar{\phi}_i(x) = \phi_i(x) + \Delta\phi_i(x) \tag{10}$$

$$\bar{\lambda}_i = \lambda_i + \Delta\lambda_i \tag{11}$$

where $\Delta\varphi_i(x)$ and $\Delta\lambda_i$ is the increment of the i^{th} eigenvalues and eigen function of the non-uniform Bernoulli-Euler beam. $\Delta\varphi_i(x)$ is consistent with a sum of the first n eigen functions of the uniform Euler-Bernoulli beam except the i^{th} eigen function $\varphi_i(x)$ and is written as follows

$$\Delta\phi_i(x) \cong \sum_{j=1, j\neq i}^{\eta} \phi_j(x) q_j \tag{12}$$

where q_j is defined as the modal linear combination coefficient. Obviously, to obtain the η unknown variables which are made up of the increment $\Delta\lambda_i$ and the coefficients q_j (j=1, 2, ⋯, η; $j\neq i$), the eigenvalues and eigen functions of the non-uniform beam with added masses and elastic supports are achievable in Eq. (10) and Eq. (11). Based on the basic structure dynamic theory (Clough and Penzien 2003, Timoshenko 1974), the uniform beam has an infinite number of normal modes and an ample number of accurate results of the eigenvalue and eigen functions, which in practice can be acquired by using a limited number of low order modes.

Substituting Eqs. (6), (7), (10) and (11) into Eq. (3), we have

$$\begin{aligned}
&EI_0\frac{\partial^4\Delta\phi_i(x)}{\partial x^4}+\frac{\partial^2}{\partial x^2}\left[\Delta EI(x)\frac{\partial^2\phi_i(x)}{\partial x^2}\right]+\frac{\partial^2}{\partial x^2}\left[\Delta EI(x)\frac{\partial^2\Delta\phi_i(x)}{\partial x^2}\right]\\
&-\big[\lambda_i\rho A_0\Delta\phi_i(x)+\lambda_i\rho\Delta A(x)\phi_i(x)+\lambda_i\rho\Delta A(x)\Delta\phi_i(x)+\Delta\lambda_i\rho A_0\phi_i(x)\\
&\qquad+\Delta\lambda_i\rho A_0\Delta\phi_i(x)+\Delta\lambda_i\rho\Delta A(x)\phi_i(x)+\Delta\lambda_i\rho\Delta A(x)\Delta\phi_i(x)\big]\\
&-\sum_{a=1}^{h+1}m_a\delta\left(x-x_a^m\right)\left[\lambda_i\phi_i(x)+\lambda_i\Delta\phi_i(x)+\Delta\lambda_i\phi_i(x)+\Delta\lambda_i\Delta\phi_i(x)\right]+\sum_{b=1}^{n+1}k_b\delta\left(x-x_b^s\right)\Delta\phi_i(x)=0
\end{aligned}\tag{13}$$

Implementing Eq. (12) into Eq. (13) and pre-multiplying both sides of the result with $\varphi_k(x)$ (k=1, 2, ⋯, η) and then integrating the final equation over the beam length, will allow simplification to occur by using the mode orthogonally (Clough and Penzien 2003). This is formulated as

$$\Delta\lambda_i\left(m_k\delta_{ki}+\Delta m_{ki}\right)+\Delta\lambda_i\sum_{j=1,j\neq i}^{\eta}\left(m_k\delta_{kj}+\Delta m_{kj}\right)q_j+\sum_{j=1,j\neq i}^{\eta}\left[\left(\lambda_i-\lambda_j\right)m_k\delta_{kj}+\left(\lambda_i\Delta m_{kj}-\Delta k_{kj}\right)\right]q_j=\Delta k_{ki}-\lambda_i\Delta m_{ki}\tag{14}$$

where

$$m_k=\int_0^L\rho A_0\phi_k^2(x)dx\tag{15}$$

$$\Delta m_{ki}=\int_0^L\rho\Delta A(x)\phi_k(x)\phi_i(x)dx+\int_0^L\sum_{a=1}^{h+1}m_a\delta\left(x-x_a^m\right)\phi_k(x)\phi_i(x)dx\tag{16}$$

$$\Delta k_{ki}=\int_0^L\phi_k(x)\frac{\partial^2}{\partial x^2}\left[\Delta EI(x)\phi_i''(x)\right]dx\tag{17}$$

Eq. (15) and Eq. (16) can be achieved directly by numerical integration whereas Eq. (17) has to be simplified first. In this paper, section **3.2** will give the simplified calculation method of Eq. (17) in elastic boundary conditions.

Eq. (14) can be written in a matrix form (k=1, 2, ⋯, η)

$$[\mathbf{A}-\mathbf{B}+\lambda_i\mathbf{C}+\lambda_i\mathbf{D}q_i]\boldsymbol{q}=\boldsymbol{p}\tag{18}$$

where the i^{th} coefficient q_i of the position vector $\boldsymbol{q}$ is $\Delta\lambda_i/\lambda_i$ and the other elements of the position vector $\boldsymbol{q}$ were consist of the modal linear combination coefficients. The matrices **A**, **B**, **C**, **D**, $\boldsymbol{p}$ and $\boldsymbol{q}$ are defined in Appendix ***A***. Thus the variable coefficient differential Eq. (1) is transformed into the nonlinear matrix Eq. (18).

4.2 The calculation of coefficient Δk_{ki} in elastic boundary condition.

Directly using Eq. (17) is more difficult to gain coefficient values Δk_{ki}, which requires simplifying Eq. (17) and indirectly gaining coefficient values Δk_{ki}. Substituting Eq. (6) into Eq. (17), we get

$$\Delta k_{ki}=\int_0^L\phi_k(x)\frac{\partial^2}{\partial x^2}\left[EI(x)\phi_i''(x)\right]dx-\int_0^L\phi_k(x)\frac{\partial^2}{\partial x^2}\left[EI_0\phi_i''(x)\right]dx\tag{19}$$

Substituting Eq. (9) into Eq. (19), we obtain

$$\Delta k_{ki}=\int_0^L\phi_k(x)\frac{\partial^2}{\partial x^2}\left[EI(x)\phi_i''(x)\right]dx-\lambda_i\int_0^L\rho A_0\phi_k(x)\phi_i(x)dx+\int_0^L\sum_{b=1}^{n+1}k_b\delta\left(x-x_b^s\right)\phi_k(x)\phi_i(x)dx \quad (20)$$

when $k\neq i$, Eq. (20) can be simplified according to the mode orthogonality

$$\Delta k_{ki}=\int_0^L\phi_k(x)\frac{\partial^2}{\partial x^2}\left[EI(x)\phi_i''(x)\right]dx+\int_0^L\sum_{b=1}^{n+1}k_b\delta\left(x-x_b^s\right)\phi_k(x)\phi_i(x)dx \quad (21)$$

According to the property of the $\delta(x)$ function, Eq. (21) can be rewritten approximately as

$$\Delta k_{ki}=\int_0^L\phi_k(x)\frac{\partial^2}{\partial x^2}\left[EI(x)\phi_i''(x)\right]dx+\sum_{b=1}^{n+1}k_b\phi_k\left(x_b^s\right)\phi_i\left(x_b^s\right) \quad (22)$$

when $k=i$, Eq. (20) can be rewritten as

$$\Delta k_{ki}=\int_0^L\phi_i(x)\frac{\partial^2}{\partial x^2}\left[EI(x)\phi_i''(x)\right]dx-\lambda_i\int_0^L\rho A_0\phi_i^2(x)dx+\sum_{b=1}^{n+1}k_b\phi_i^2\left(x_b^s\right) \quad (23)$$

The first item of Eq. (20) can be rewritten as follows by subsection integration

$$\int_0^L\phi_k(x)\frac{\partial^2}{\partial x^2}\left[EI(x)\phi_i''(x)\right]dx=\phi_k(x)\frac{\partial}{\partial x}\left[EI(x)\phi_i''(x)\right]\Bigg|_0^L-\phi_k'(x)EI(x)\phi_i''(x)\Big|_0^L+\int_0^L EI(x)\phi_i''(x)\phi_k''(x)dx$$

(24)

Apparently, the first item of Eq. (24) shows that the boundary shear of the i^{th} mode shape works on the displacement of the k^{th} mode shape and the second item of Eq. (24) expresses that boundary bending moment of the i^{th} mode shape works on the rotating angle of the k^{th} mode shape. For the uniform beam with elastic supports, the second item of Eq. (24) is always zero. Eq. (24) can be written as follows

$$\int_0^L\phi_k(x)d\frac{\partial}{\partial x}\left[EI(x)\phi_i''(x)\right]=\phi_k(x)\frac{\partial}{\partial x}\left[EI(x)\phi_i''(x)\right]\Bigg|_0^L+\int_0^L EI(x)\phi_k''(x)\phi_i''(x)dx \quad (25)$$

As shown in Fig. 1(d), the boundary conditions of the uniform beam with elastic supports are

$$-k_1\phi(0)=EI_0\phi'''(0) \quad (27)$$

$$k_{n+1}\phi(L)=EI_0\phi'''(L) \quad (28)$$

Substituting Eqs. (27) and (28) into Eq. (25), we get

$$\int_0^L\phi_k(x)d\frac{\partial}{\partial x}\left[EI(x)\phi_i''(x)\right]=k_{n+1}\phi_k(L)\phi_i(L)+k_1\phi_k(0)\phi_i(0)+\int_0^L EI(x)\phi_k''(x)\phi_i''(x)dx \quad (29)$$

According to Eq. (22), Eq. (23) and Eq. (29), Eq. (19) can be modified

$$\Delta k_{ki}=\begin{cases}\int_0^L EI(x)\phi_k''(x)\phi_i''(x)dx+\sum_{b=1}^{n+1}k_b\phi_k\left(x_b^s\right)\phi_i\left(x_b^s\right)+k_1\phi_k(0)\phi_i(0)+k_{n+1}\phi_k(L)\phi_i(L) & k\neq i\\ \int_0^L EI(x)\left[\phi_i''(x)\right]^2dx+\sum_{b=1}^{n+1}k_b\phi_i^2\left(x_b^s\right)-\lambda_i\int_0^L\rho A_0\phi_i^2(x)dx+k_1\phi_i^2(0)+k_{n+1}\phi_i^2(L) & k=i\end{cases} \quad (30)$$

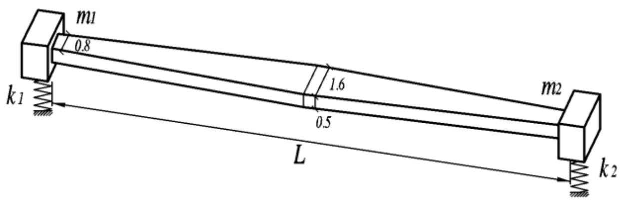

Fig. 2 single-span beam (Unit: m)

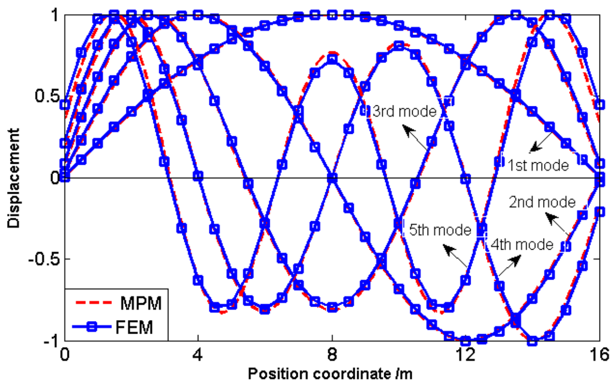

Fig. 3 The first five mode shapes

Eventually, coefficient Δk_{ki} can be obtained easily using Eq. (30).

4.3 To solve the nonlinear algebraic equations.

Eq. (18) can be solved by Newton-Ralph method and genetic algorithm, etc (Burden and Faires 1997). Because the Jacobian matrix of Eq. (18) can be acquired easily, Eq. (18) are solved directly by Newton-Raphson method in this paper. It is very important to select initial value for Newton-Raphson method. Appropriate initial value can not only reduce the number of iterations but also obtain more accurate results. According to the physical meaning of Eq. (18) and combination coefficient $\boldsymbol{q}$, the initial value is given as

$$\boldsymbol{q=0} \tag{31}$$

The iteration of terminal condition is (Lou and Wu 1997)

$$\left|q_i^{(\kappa)} - q_i^{(\kappa-1)}\right| \Big/ \left|q_i^{(\kappa)}\right| \le \xi \tag{32}$$

where κ is the number of iterations and ξ is the convergent error.

When the vector $\boldsymbol{q}$ has been obtained, the i^{th} mode shape and natural frequency of the non-uniform beam with added masses and elastic supports can be acquired from Eqs. (10) and (11). Make the i in Eqs. (10) and (11) equals to 1, 2, $\cdots$, n and repeat the above iterative process, the first n order modal parameters of the non-uniform Bernoulli-Euler beam with added masses and elastic supports can be gained.

Table 1 The natural frequencies of the single-span beam (Unit: HZ)

Freq.	FEM	MPM							
		η=6	η=7	η=8	η=9	η=10	η=11	η=12	η=13
f_1	4.43022	4.45612(3)[a]	4.45472(3)	4.45472(3)	4.45243(3)	4.45243(3)	4.45197(3)	4.45197(3)	4.45156(3)
f_2	17.64774	17.85962(4)	17.85962(3)	17.82835(3)	17.82835(3)	17.80986(3)	17.80986(3)	17.80372(3)	17.80372(3)
f_3	39.58707	40.52119(4)	40.31455(4)	40.31455(4)	40.20429(4)	40.20429(4)	40.14510(4)	40.14510(4)	40.12668(4)
f_4	69.22859	72.08915(3)	72.08915(3)	71.47583(4)	71.47583(4)	71.24049(4)	71.24049(4)	71.13326(4)	71.13308(4)
f_5	109.30385	113.26756(4)	112.12905(4)	112.12905(4)	111.00607(4)	1.1100607(4)	110.68292(4)	110.68292(4)	110.50141(4)

a. Number in bracket shows the number of iterations, which has the same meaning in the Table 2.

5. Examples and discussion

5.1 Single-span beam with added masses and elastic supports.

A single-span beam with added masses and elastic supports is shown in Fig. 2. The beam was made of mild steel of cross-sectional area from 0.5 m×0.8 m to 0.5 m×1.6 m with a length of 16 m. It had the following material properties: Young's modulus E=200 GPa, density ρ=7850 kg/m^3, added mass m_1=m_2=2000 kg, supports stiffness k_1=k_2=5×10^6 kN/m, convergent error ξ=1×10^{-8}. The natural frequencies of the single-span beam which were obtained by the MPM and the finite element method (FEM), are shown in Table 1. The first five mode shapes acquired by the MPM (η=9) and FEM are shown in Fig. 3.

5.2 Two-span stepped beam with elastic supports.

A two-span stepped beam with elastic supports is shown in Fig. 4. Stepped beam with elastic supports was made of mild steel of cross-sectional area from 0.3 m×0.5 m to 0.3 m×0.3 m with a length of L_1=L_2=5 m. It had the following material properties: Young's modulus E=200 GPa, density ρ=7850 kg/m^3, supports stiffness k_1=k_2=k_3=2.0×10^7 kN/m, convergent error ξ=1×10^{-8}. The natural frequencies and the first five mode shapes of the two-span stepped beam, which are obtained by the MPM (η=9), ADM (Mao 2011) and FEM, are shown in Table 2 and Fig. 5, respectively.

In Table 1 and Table 2, the natural frequencies obtained by MPM are well agreed with the results of FEM and ADM. The results show that the bigger the value of η has the more accurate this method results are. Obviously, the modal parameters of non-uniform Bernoulli-Euler beam with added masses and elastic supports can be obtained enough accuracy by extending the application of the modal perturbation method. The MPM results are slightly greater than the results of ADM and FEM because it's belongs to the Ritz method (Clough and Penzien 2003) and the results of the Ritz method are always higher than the real frequencies based on dynamics of structures. The MPM has the advantages of rapid convergence and high precision according to the iterative times and the frequency results in Table 1 and Table 2. At the same time the mode shapes of the single-span beam and two-span stepped beam obtained by the MPM are also consistent well with the FEM and ADM results. By comparing the modal displacement in elastic supports in Fig. 3 and Fig. 5, the MPM can effectively consider the effects of the dynamic characteristic with the elastic supports.

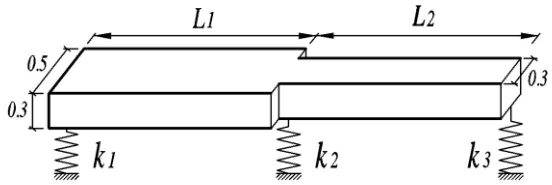

Fig. 4 Two-span stepped beam (Unit: m)

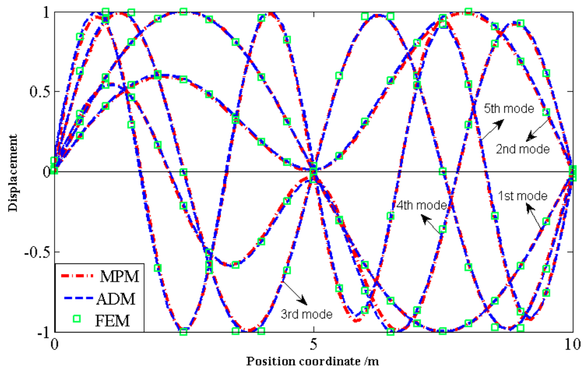

Fig. 5 The first five mode shapes

Table 2 The natural frequencies of two-span stepped beam (Unit: Hz)

Freq.	ADM	FEM	MPM						
			η=7	η=8	η=9	η=10	η=11	η=12	η=13
f_1	26.75217	26.74879	26.76252(3)	26.76230(3)	26.76223(3)	26.76220(3)	26.76220(3)	26.76219(3)	26.76219(3)
f_2	41.60236	41.61601	41.78257(4)	41.78189(4)	41.78167(4)	41.79841(4)	41.77116(4)	41.76831(4)	41.76692(4)
f_3	106.78979	106.73371	106.95582(4)	106.95459(4)	106.95421(4)	106.95403(4)	106.94919(4)	106.94001(3)	106.93796(4)
f_4	133.18575	133.33598	134.08198(4)	134.07538(4)	134.07345(4)	134.07253(4)	134.01742(4)	1.3400933(4)	133.99695(4)
f_5	239.42214	239.09972	240.28674(4)	240.26261(4)	240.25795(4)	240.25597(4)	240.23056(4)	240.22065(3)	240.21968(4)

The MPM can accurately and efficiently obtain the modal parameters of the structure with the basic information, such as material, cross section and span length but FEM need not only the above information but also the geometric modeling and meshing. Calculation accuracy of the FEM is related to the grid quality and size. The computing power is about the number of elements. Furthermore, FEM need to manually adjust the parameter values in the parameter sensitivity analysis and the computation efficiency is low. Conversely, the method of this paper can do parameter sensitivity analysis conveniently. Obviously, it has the incomparable advantage over FEM in the computation efficiency and parameter sensitivity analysis.

As shown in Table 1, when solving the odd-order modal parameters, the results of η=2n+1 (n=2, 3, ⋯) is comparatively close with the results of η=2n+2. Solving the even-order modal parameters, the results of η=2n+1(n=2, 3, ⋯) and the results of η=2n are also comparatively close. This shows that the even-order modal has less of an influence on the results of the odd-order modal parameters and the odd-order modal also has less of an influence on the results of the even-order modal parameters. This conclusion, though, does not apply to case 2 in section **5.2**. This is associated with the symmetry of structure and section 5 in this paper will present a detailed discussion about this law.

6. A simplified method for symmetrical beam

6.1 Simplified method and formula.

According to the symmetry of mode shape and the value of modal linear combination coefficient q_j, Eq. (18) can be simplified. Based on the dynamics of structures (Clough and Penzien 2003), the odd-order mode shapes of the symmetrical beam have the same symmetry and the even-order mode shapes of the symmetrical beam have the same symmetry, but the odd-order mode shapes and the even-order mode shapes always have the opposite symmetry. The even-order mode shapes of the uniform beam, which have the opposite symmetry of the odd-order mode shapes will interfere with the solution of the odd-order modal parameters of the non-uniform beam and will increase the number of iterations and reduce the convergence speed. Therefore, we can only use the odd-order mode shapes of the uniform beam and ignore the influence of even-order mode shapes to solve the odd-order modal parameters of the non-uniform beam. If using the first η^{th} mode shapes (assuming that the value of η is an odd number) of the uniform beam to solve the odd-order modal parameters of the non-uniform beam, then Eq. (18) can be simplified to

$$[\mathbf{A_s}-\mathbf{B_s}+\lambda_i\mathbf{C_s}+\lambda_i\mathbf{D_s}q_{si}]\boldsymbol{q_s}=\boldsymbol{p_s} \tag{33}$$

The matrices $\mathbf{A_s}$, $\mathbf{B_s}$, $\mathbf{C_s}$, $\mathbf{D_s}$, $\mathbf{p_s}$ and $\mathbf{q_s}$ are defined in Appendix ***B***. Apparently, the nonlinear algebraic Eq. (18) with η unknown numbers have been transformed into the Eq. (34) with $(\eta+1)/2$ unknown numbers.

Similarly, the even-order modal parameters of the non-uniform beam can be obtained only with the even-order mode shapes of uniform beam. When using the first η^{th} mode shapes (assuming that the value of η is an even number) of the uniform beam to solve the even-order modal parameters of the non-uniform beam, Eq. (18) can also be simplified and the matrices $\mathbf{A_s}$, $\mathbf{B_s}$, $\mathbf{C_s}$, $\mathbf{D_s}$, $\mathbf{p_s}$ and $\mathbf{q_s}$ are also defined in Appendix ***B***.

In the same way, the nonlinear algebraic Eq. (18) with η unknown numbers have been transformed into the Eq. (33) with $\eta/2$ unknown numbers. This method can be called the simplified modal perturbation method (SMPM).

6.2 Simplified calculation verification & Example 1.

Taking a pedestrian beam bridge as an example, the symmetrical beam bridge is shown in Fig. 6. Using SMPM and MPM to solve the modal parameters, respectively, the results are shown in Table 3 and Table 4. Limited by space, the paper only gives the results of the first two frequencies. beam length is 20 m, concrete grade is C50, the bottom edge and top floor of the beam changed as the quadratic parabola, added mass in supports is 4100 kg, added mass in the midspan is 1920 kg; supports stiffness is about 7.6×10^6 kN/m and convergent error is $\xi=1\times10^{-8}$.

Example 2.

Two-span continuous beam bridge is shown in Fig. 8, span length is 50 m+50 m, concrete grade is C50, the bottom edge and top floor of the beam changed as the quadratic parabola, added

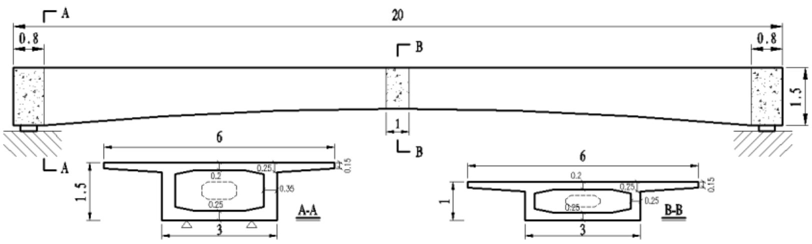

Fig. 6 The general layout of the pedestrian bridge (Unit: m)

Table 3 The perturbation results of fundamental frequency

	η	5 (MPM)[b]	5 (SMPM)	7 (MPM)	7 (SMPM)	9 (MPM)	9 (SMPM)	11 (MPM)	11 (SMPM)
	1st freq.	5.49609(3)[c]	5.49609(3)	5.49597(3)	5.49597(3)	5.49597(3)	5.49597(3)	5.49597(3)	5.49597(3)
	q_1	-0.25699	-0.25699	-0.25703	-0.25702	-0.25703	-0.25702	-0.25703	-0.25702
	q_2	-0.00006	-	-0.00006	-	-0.00006	-	-0.00006	-
	q_3	-0.34590	-0.34590	-0.34574	-0.34574	-0.34574	-0.34574	-0.34574	-0.34574
	q_4	-0.00034	-	-0.00027	-	-0.00027	-	-0.00027	-
	q_5	-0.09732	-0.09732	-0.09285	-0.09285	-0.09286	-0.09285	-0.09285	-0.09285
$\boldsymbol{q}$	q_6	-	-	-0.00060	-	-0.00052	-	-0.00054	-
	q_7	-	-	-0.02400	-0.02399	-0.02406	-0.02405	-0.02403	-0.02405
	q_8	-	-	-	-	-0.00032	-	-0.00030	-
	q_9	-	-	-	-	0.00023	0.00022	0.00029	0.00025
	q_{10}	-	-	-	-	-	-	-0.00010	-
	q_{11}	-	-	-	-	-	-	0.00002	-0.00010

b. The title in bracket shows the computing method, which has the same meaning in the Table 4-Table 6.
c. Number in bracket shows the number of iterations, which has the same meaning in the Table 4-Table 6.

Table 4 The perturbation results of second frequency

	η	6 (MPM)	6 (SMPM)	8 (MPM)	8 (SMPM)	10 (MPM)	10 (SMPM)	12 (MPM)	12 (SMPM)
	2nd freq.	24.21885(4)	24.37514(3)	24.21881(3)	24.37111(3)	24.21879(3)	4.21879(3)	24.21878(3)	24.21878(3)
	q_1	0.00000	-	0.00000	-	0.00000	-	0.00000	-
	q_2	-0.06911	-0.05706	-0.06912	-0.05737	-0.06912	-0.06911	-0.06912	-0.06911
	q_3	-0.00001	-	-0.00001	-	-0.00001	-	-0.00001	-
	q_4	-0.30293	-0.32325	-0.30293	-0.32252	-0.30292	-0.30292	-0.30292	-0.30291
	q_5	-0.00002	-	-0.00001	-	-0.00001	-	-0.00001	-
	q_6	-0.05690	-0.12212	-0.05621	-0.11419	-0.05622	-0.05622	-0.05622	-0.05622
$\boldsymbol{q}$	q_7	-	-	-0.00001	-	-0.00001	-	-0.00001	-
	q_8	-	-	-0.00299	-0.03717	-0.00323	-0.00322	-0.00325	-0.00325
	q_9	-	-	-	-	-0.00001	-	0.00000	-
	q_{10}	-	-	-	-	0.00094	0.00093	0.00083	0.00083
	q_{11}	-	-	-	-	-	-	0.00000	-
	q_{12}	-	-	-	-	-	-	0.00050	0.00048

mass on side support is 20215 kg, added mass on the intermediate support is 53220 kg; side support stiffness is about 1.68×10^7 kN/m, intermediate support stiffness is about 5.1×10^7 kN/m and convergent error is $\zeta=1\times10^{-8}$. The results of the first two frequencies by SMPM and MPM are shown in Table 5 and Table 6.

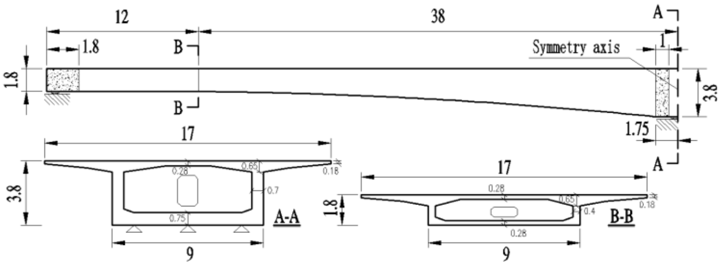

Fig. 7 The general layout of two-span continuous beam (Unit: m)

Table 5 The perturbation results of fundamental frequency

	η	5 (MPM)	5 (SMPM)	7 (MPM)	7 (SMPM)	9 (MPM)	9 (SMPM)	11 (MPM)	11 (SMPM)
1st freq.		1.90414(4)	1.90426(4)	1.90376(4)	1.90391(4)	1.90234(4)	1.90255(4)	1.90212(4)	1.90241(4)
	q_1	-0.30457	-0.30448	-0.30485	-0.30473	-0.30588	-0.30572	-0.3060	-0.30583
	q_2	-0.00458	-	-0.00396	-	-0.00325	-	-0.00272	-
	q_3	0.374024	0.37390	0.37659	0.37634	0.37801	0.37761	0.37846	0.37791
	q_4	-0.01498	-	-0.01649	-	-0.01428	-	-0.01313	-
	q_5	-0.20250	-0.20272	-0.20898	-0.20952	-0.19794	-0.19863	-0.19686	-0.19790
$\boldsymbol{q}$	q_6	-	-	-0.01199	-	-0.01397	-	-0.00949	-
	q_7	-	-	-0.04943	-0.05031	-0.06040	-0.06140	-0.06044	-0.06126
	q_8	-	-	-	-	-0.02471	-	-0.02384	-
	q_9	-	-	-	-	-0.12983	-0.13079	-0.13023	-0.13090
	q_{10}	-	-	-	-	-	-	-0.03575	-
	q_{11}	-	-	-	-	-	-	-0.04190	-0.04573

Table 6 The perturbation results of second frequency

	η	6 (MPM)	6 (SMPM)	8 (MPM)	8 (SMPM)	10 (MPM)	10 (SMPM)	12 (MPM)	12 (SMPM)
2nd freq.		3.85903(3)	3.85958(3)	3.85373(3)	3.85414(3)	3.85362(3)	3.85398(4)	3.84139(4)	3.85348(4)
	q_1	0.00143	-	0.00109	-	0.00119	-	0.00074	-
	q_2	0.18133	0.18167	0.17809	0.17834	0.17802	0.17825	0.17056	0.17794
	q_3	-0.00727	-	-0.00414	-	-0.00368	-	-0.00171	-
	q_4	0.53752	0.54245	0.54835	0.54841	0.54386	0.54735	0.54665	0.54790
	q_5	-0.03375	-	-0.03650	-	-0.03459	-	-0.02659	-
	q_6	-0.18518	-0.18474	-0.20166	-0.20318	-0.20160	-0.20481	-0.18150	-0.20368
$\boldsymbol{q}$	q_7	-	-	-0.06197	-	-0.06373	-	-0.02557	-
	q_8	-	-	-0.11725	-0.14695	-0.11704	-0.14477	-0.11854	-0.14428
	q_9	-	-	-	-	-0.01686	-	-0.05221	-
	q_{10}	-	-	-	-	-0.01594	0.03049	0.023437	0.03079
	q_{11}	-	-	-	-	-	-	-0.30317	-
	q_{12}	-	-	-	-	-	-	-0.06311	-0.06859

Form Table 3-Table 6, the first two frequencies of SMPM is very close to the results of MPM for the symmetrical beams. The iterations of SMPM are not significant more increase than that of MPM. Comparison the other-order frequencies of SMPM with that of MPM, This law is also established. This shows that the odd-order modal parameters of the symmetrical non-uniform beam can be obtained by using the SMPM while ignoring the influence of the even-order mode shapes to gain the results. Also, the even-order modal parameters of the non-uniform beam can also be acquired by using the SMPM while only considering the influence of the even-order mode shapes to gain the results. In conclusion, the SMPM can solve the modal parameters of the symmetrical non-uniform beam as well as calculate the accuracy to be very close to the MPM. However, the SMPM as about half the number of coefficients and unknowns as does the MPM. Therefore, the SMPM computational efficiency is greater.

7. The effects of added mass and support stiffness

Three-span continuous beam bridge is shown in Fig. 8. Size and location of added mass and support stiffness, which effect on the dynamic characteristics of the three-span continuous beam bridge, are been studied by this method. Span length is 38 m+60 m+38 m, concrete grade is C50, the bottom edge and top floor of the beam changed as the quadratic parabola, added mass on the side support and midspan is 23500 kg, added mass on the intermediate support is 48000 kg; side support stiffness is about 9.0×10^7 kN/m, intermediate support stiffness is about 2.7×10^7 kN/m and convergent error is $\xi=1\times10^{-8}$.

7.1 The effect of the size of added mass and support stiffness.

In modal analysis, eight conditions are shown in Table 7 according to whether to consider the support stiffness and added mass. First six frequencies of each condition are been calculated by MPM (η=9).

From Table 7, the results of condition 1 are different with that of condition 5. It shows that the added mass and support stiffness effect on the natural frequencies and the high-order natural frequencies have higher sensitivity than the low-order natural frequencies. Condition 1 and condition 3 have quite close results. Condition 2 and condition 4 also have similar results. It can be inferred that added mass on hinged bearing effect on the frequencies is very weak. The results of condition 1 are different from condition 4. It can be concluded that added mass in midspan effects

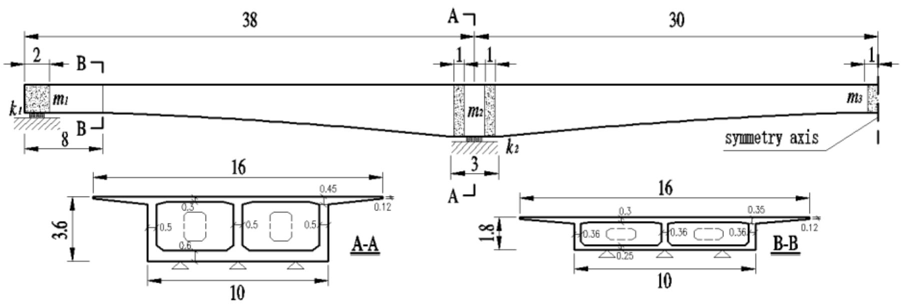

Fig. 8 The general layout of three-span continuous beam bridge (Unit: m)

Table 7 Frequencies of three-span continuous beam bridge in each condition

Condition		1	2	3	4	5	6	7	8
Support stiffness kN/m	k_1	o[d]	o	o	o	9×10^6	9×10^6	9×10^6	9×10^6
	k_2	o	o	o	o	2.7×10^7	2.7×10^7	2.7×10^7	2.7×10^7
	k_3	o	o	o	o	2.7×10^7	2.7×10^7	2.7×10^7	2.7×10^7
	k_4	o	o	o	o	9×10^6	9×10^6	9×10^6	9×10^6
Added mass kg	m_1	0	23500	23500	0	23500	0	23500	0
	m_2	0	48000	48000	0	48000	0	48000	0
	m_3	0	23500	0	23500	23500	0	0	23500
	m_4	0	48000	48000	0	48000	0	48000	0
	m_5	0	23500	23500	0	23500	0	23500	0
Frequency Hz	f_1	2.06383	2.03355	2.06383	2.03354	2.02833	2.05856	2.05855	2.02834
	f_2	3.96812	3.96812	3.96812	3.96812	3.94851	3.94854	3.94851	3.94854
	f_3	5.38605	5.34368	5.38605	5.34367	5.26184	5.30220	5.30202	5.26201
	f_4	8.34615	8.34615	8.34615	8.34614	8.17638	8.17724	8.17638	8.17724
	f_5	13.35731	13.21745	13.35731	13.21745	13.10949	13.24843	13.24638	13.11141
	f_6	15.98634	15.98628	15.98634	15.98628	15.33352	15.34691	15.33366	15.34684

d. “o” shows the hinged bearing and the stiffness of hinged bearing is infinite value.

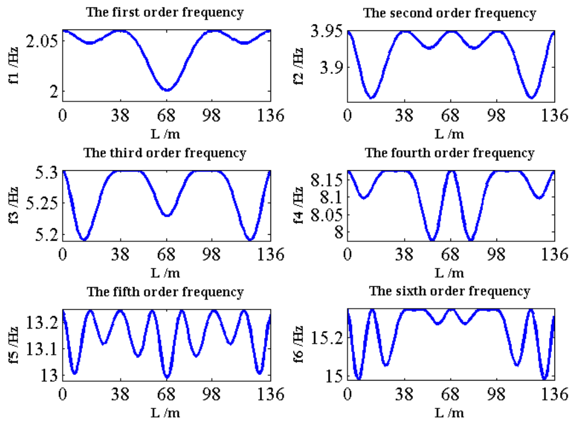

Fig. 9 The effect of added mass m6 in different location on the natural frequencies

on the frequencies, and it is not to be ignored. The results of condition 6 and 7 are less than that of condition 1 and 3. It can be seen that the added mass on elastic support can be considered on dynamic characteristic when the support stiffness is been given. The results of condition 8 are larger than that of condition 5. This shows that the actual support stiffness in bridge is a high value but the added mass on bearing will have greater effect on the dynamic characteristic when support is damaged.

7.2 The effect of location of added mass.

The different location added mass has the different effect on the dynamic characteristic of the bridge. Added mass m_6 (m_6=m_2) in different location is studied. The results are shown in Fig. 9.

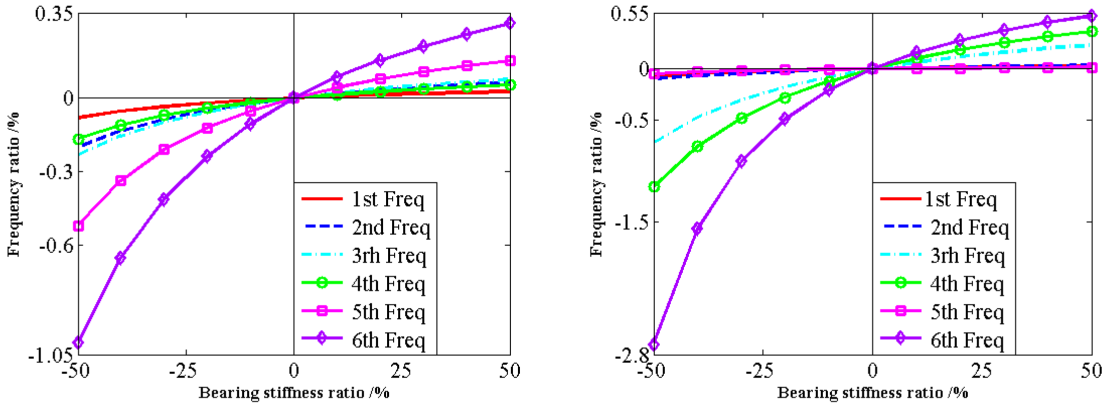

(a) Side support (b) Intermediate support

Fig. 10 The first six natural frequencies versus the change of one support stiffness

From Fig. 9, the added mass m_6 has the different effect on the different order natural frequencies. The added mass m_6 on the midspan of the main span and side span has a greater influence on the fundamental frequency. The added mass m_6 on the midspan of the main span has a significant impact on the odd-order natural frequencies and almost no effect on the even-order natural frequencies. Analysis shows that this is associated with the symmetry of mode shapes. The added mass m_6 on the support has trifling impact on the natural frequencies.

7.3 The effect of support stiffness.

With the increase of the bridge service life, bridge support will appear different damage under long-term load and environmental factors. Under the accidental loading factors, bridge support will appear failure. These will cause the decline of support stiffness with varying degrees. The first six natural frequencies versus the change of one support stiffness (±50%), which stands for the different damage degree of bridge support, is shown in Fig. 10.

From Fig. 10, with the increase of support stiffness, natural frequencies increased slightly with nonlinear relationship. Because the actual support stiffness of bridges is generally larger and natural frequencies only slightly increase with the increase of support stiffness. Conversely, when the bridge support has a damage, Natural frequencies will have obvious decline with the decrease of support stiffness. The change of intermediate support stiffness has the more significant effect on natural frequencies than that of side support stiffness. Preliminary analysis suggests that these are caused by the relatively large variation of the intermediate support stiffness. Generally, high-order natural frequencies has higher sensitivity than lower-order natural frequencies with the change of support stiffness but the change of individual order natural frequency don't meet this rule, such as the fourth-order natural frequency in Fig. 10(a) and the fifth-order natural frequency in Fig. 10(b). By looking for the frequency which has the higher sensitivity of support damage, we can do the support damage identification research using the analytical solution of dynamic characteristics of non-uniform beam with added masses and elastic supports.

7. Conclusions

In this paper, the free vibration of the non-uniform Euler–Bernoulli beam with arbitrary added masses and elastic supports are analyzed by extending the application of the modal perturbation method. This method can not only solve the free vibration of the complicated beam (Lou and Wu 1997) but also consider the added mass on the support and support stiffness effects on the dynamic characteristics of the beam effectively. It's adapted for calculating the dynamic characteristics of non-uniform beam bridge. The specific calculation formula of Δk_{ki} is deduced in the elastic boundary conditions. The results of this paper are in excellent agreement with published results. The solution can be obtained by solving a set of nonlinear algebraic equations with unknown numbers. The MPM results are slightly greater than the real results because it's belongs to the Ritz method. The MPM has the incomparable advantage over the FEM in the parameter sensitivity analysis and computation efficiency.

Furthermore, SMPM can reduce the coefficients and unknown numbers of about 50% and the number of iterations is not increased significantly. The computational efficiency of SMPM is higher than that of MPM for the symmetrical non-uniform beam.

Using the analytical solution of dynamic characteristics of non-uniform beam with added masses and elastic supports, the effects of size and location of added mass and support stiffness on the dynamic characteristics of three-span continuous beam bridge have been studied.

Acknowledgments

This work is partially supported by Natural Science Foundation of China under Grant no. 51378039 and 51378037 by the Beijing Lab of Earthquake Engineering and Structural Retrofit, Foundation of Key Laboratory of Urban Security and Disaster Engineering, Ministry of Education under Grant no. USDE2014032.

References

Bahrami, M.N., Arani, M.K. and Saleh, N.R. (2011), "Modified wave approach for calculation of natural frequencies and mode shapes in arbitrary non-uniform beams", *Scientia Iranica*, **18**(5), 1088-1094.

Bambill, D.V., Rossit, C.A., Rossi, R.E., Felix, D.H. and Ratazzi, A.R. (2013), "Transverse free vibration of non uniform rotating Timoshenko beams with elastically clamped boundary conditions", *Meccanica*, **48**(6), 1289-1311.

Bedon, C. and Morassi, A. (2014), "Dynamic testing and parameter identification of a base-isolated bridge", *Eng. Struct.*, **60**(1-2), 85-99.

Burden, R.L. and Faires, J.D. (1997), *Numerical Analysis, sixth edition*, Brooks Cole Publishing Company, Pacific Grove, California, USA.

Chen, D.W. and Wu, J.S. (2002), "The exact solution for the natural frequencies and mode shapes of non-uniform beams with multiple spring-mass systems", *J. Sound Vib.*, **255**(2), 299-322.

Clough, R.W. and Penzien, J. (2003), *Dynamics of Structures, second edition*, Computers and Structures, New York, USA.

DeRosa, M.A., Franciosi, C. and Maurizi, M.J. (1996), "On the dynamic behavior of slender beams with elastic ends carrying a concentrated mass", *Comput. Struct.*, **58**(6), 1145-1159.

Elishakoff, I. and Johnson, V. (2005), "Apparently the first closed-form solution of vibrating inhomogeneous beam with a tip mass", *J. Sound Vib.*, **286**(4-5), 1057-1066.

Kamke, E. (1980), *Ordinary Differential Equation Manual*, Science Press, Beijing, China.

Firouz-Abadi, R.D., Haddadpour, H. and Novinzadeh, A.B. (2007), "An asymptotic solution to transverse free vibrations of variable-section beams", *J. Sound Vib.*, **304**(3-5), 530-540.

Ho, S.H. and Chen, C.K. (1998), "Analysis of general elastically end restrained non-uniform beams using differential transform", *Appl. Math. Model.*, **22**(4-5), 219-234.

Hsu, J.C., Lai, H.Y. and Chen, C.K. (2008), "Free vibration of non-uniform Euler-Bernoulli beams with general elastically end constraints using Adomian modified decomposition method", *J. Sound Vib.*, **318**(4-5), 965-981.

Huang, Y. and Li, X.F. (2010), "A new approach for free vibration of axially functionally graded beams with non-uniform cross-section", *J. Sound Vib.*, **329**(11), 2291-2303.

Pratiher, B. (2012), "Vibration control of a transversely excited cantilever beam with tip mass", *Arch. Appl. Mech.*, **82**(1), 31-42.

Jovanovic, V. (2011), "A Fourier series solution for the transverse vibration response of a beam with a viscous boundary", *J. Sound Vib.*, **330**(7), 1504-1515.

Lee, S.Y. and Yhim, S.S. (2005), "Dynamic behavior of long-span box girder bridges subjected to moving loads: numerical analysis and experimental verification", *Int. J. Solid. Struct.*, **42**(18-19), 5021-5035.

Lou, M.L., Duan, Q.H. and Chen, G. (2005), "Modal perturbation method for the dynamic characteristics of Timoshenko beams", *Shock Vib.*, **12**(6), 425-434.

Lou, M.L. and Wu, J.N. (1997), "An approach solve dynamic problems of complicated beams", *Shanghai J. Mech.*, **18**(3), 234-240.

Mao, Q.B. (2011), "Free vibration analysis of multiple-stepped beams by using Adomian decomposition method", *Math. Comput. Model.*, **54**(1), 756-764.

Sarkar, K. and Ganguli, R. (2013), "Closed-form solutions for non-uniform Euler-Bernoulli free-free beams", *J. Sound Vib.*, **332**(23), 6078-6092.

Pan, D.G., Chen, G.D. and Lou, M.L. (2012), "A modified modal perturbation method for vibration characteristics of non-prismatic Timoshenko beams", *Struct. Eng. Mech.*, **40**(5), 689-703.

Qian, B. and Yue, H.Y. (2011), "Numerical calculation of natural frequency of transverse vibration of non-uniform beam", *Mech. Eng.*, **33**(6), 45-49.

Timoshenko, S. (1974), *Vibration Problems in Engineering, fourth edition*, John Wiley& Sons, New York, USA.

Xia, J., Zhu, M.C. and Ma, D.Y. (2000), "Analysis of lateral natural vibration of beams with lumped masses and elastic supports", *Mech. Eng.*, **22**(5), 27-30.

Yang, M.J., Qiao, P.Z., McLean, D.I. and Khaleghi, B. (2010), "Effects of overheight truck impacts on intermediate diaphragms in prestressed concrete bridge girders", *PCI J.*, **55**(1), 58-78.

CC

Appendix A

The definition of different matrices used in Eq. (18) is as

$$A=\begin{bmatrix} m_1(\lambda_i-\lambda_1) & & & 0 \\ & m_2(\lambda_i-\lambda_2) & & \\ & & \ddots & \\ 0 & & & m_\eta(\lambda_i-\lambda_\eta) \end{bmatrix}_{\eta\times\eta},\ B=\begin{bmatrix} \Delta k_{11} & \cdots & \Delta k_{1\,i-1} & 0 & \Delta k_{1\,i+1} & \cdots & \Delta k_{1\eta} \\ \Delta k_{21} & \cdots & \Delta k_{2\,i-1} & 0 & \Delta k_{2\,i+1} & \cdots & \Delta k_{2\eta} \\ \vdots & \vdots & \vdots & \vdots & \vdots & \vdots & \vdots \\ \vdots & \vdots & \vdots & \vdots & \vdots & \vdots & \vdots \\ \Delta k_{\eta 1} & \cdots & \Delta k_{\eta\,i-1} & 0 & \Delta k_{\eta\,i+1} & \cdots & \Delta k_{\eta\eta} \end{bmatrix}_{\eta\times\eta},\ q=\begin{bmatrix} q_1 \\ q_2 \\ \vdots \\ q_\eta \end{bmatrix}_{1\times\eta},$$

$$C=\begin{bmatrix} \Delta m_{11} & \Delta m_{12} & \cdots & \Delta m_{1\eta} \\ \Delta m_{21} & \Delta m_{22} & \cdots & \Delta m_{2\eta} \\ \vdots & \vdots & \vdots & \vdots \\ \Delta m_{\eta 1} & \Delta m_{\eta 2} & \cdots & \Delta m_{\eta\eta} \end{bmatrix}_{\eta\times\eta},\ D=\begin{bmatrix} m_1+\Delta m_{11} & \Delta m_{12} & \cdots & 0 & \cdots & \Delta m_{1\eta} \\ \Delta m_{21} & m_2+\Delta m_{22} & \cdots & 0 & \cdots & \Delta m_{2\eta} \\ \vdots & \vdots & \vdots & \vdots & \vdots & \vdots \\ \Delta m_{i1} & \Delta m_{i2} & \cdots & 0 & \cdots & \Delta m_{i\eta} \\ \vdots & \vdots & \vdots & \vdots & \vdots & \vdots \\ \Delta m_{\eta 1} & \Delta m_{\eta 2} & \cdots & 0 & \cdots & \Delta m_{\eta\eta} \end{bmatrix}_{\eta\times\eta},\ p=\begin{bmatrix} \Delta k_{1\,i}-\lambda_i\Delta m_{1\,i} \\ \Delta k_{2\,i}-\lambda_i\Delta m_{2\,i} \\ \vdots \\ \Delta k_{\eta\,i}-\lambda_i\Delta m_{\eta\,i} \end{bmatrix}_{\eta\times 1}.$$

Appendix B

The definition of different matrices used in Eq. (33) to solve the odd-order modal parameters of the non-uniform beam is as

$$A_s=\begin{bmatrix} m_1(\lambda_i-\lambda_1) & & & 0 \\ & m_3(\lambda_i-\lambda_3) & & \\ & & \ddots & \\ 0 & & & m_\eta(\lambda_i-\lambda_\eta) \end{bmatrix}_{\frac{\eta+1}{2}\times\frac{\eta+1}{2}},\ B_s=\begin{bmatrix} \Delta k_{11} & \cdots & \Delta k_{1\,i-2} & 0 & \Delta k_{1\,i+2} & \cdots & \Delta k_{1\eta} \\ \Delta k_{31} & \cdots & \Delta k_{3\,i-2} & 0 & \Delta k_{3\,i+2} & \cdots & \Delta k_{3\eta} \\ \vdots & \vdots & \vdots & \vdots & \vdots & \vdots & \vdots \\ \vdots & \vdots & \vdots & \vdots & \vdots & \vdots & \vdots \\ \Delta k_{\eta 1} & \cdots & \Delta k_{\eta\,i-2} & 0 & \Delta k_{\eta\,i+2} & \cdots & \Delta k_{\eta\eta} \end{bmatrix}_{\frac{\eta+1}{2}\times\frac{\eta+1}{2}},$$

$$C_s=\begin{bmatrix} \Delta m_{11} & \Delta m_{13} & \cdots & \Delta m_{1\eta} \\ \Delta m_{31} & \Delta m_{33} & \cdots & \Delta m_{3\eta} \\ \vdots & \vdots & \vdots & \vdots \\ \Delta m_{\eta 1} & \Delta m_{\eta 3} & \cdots & \Delta m_{\eta\eta} \end{bmatrix}_{\frac{\eta+1}{2}\times\frac{\eta+1}{2}},\ D_s=\begin{bmatrix} m_1+\Delta m_{11} & \Delta m_{13} & \cdots & 0 & \cdots & \Delta m_{1\eta} \\ \Delta m_{31} & m_3+\Delta m_{33} & \cdots & 0 & \cdots & \Delta m_{3\eta} \\ \vdots & \vdots & \vdots & \vdots & \vdots & \vdots \\ \Delta m_{i1} & \Delta m_{i3} & \cdots & 0 & \cdots & \Delta m_{i\eta} \\ \vdots & \vdots & \vdots & \vdots & \vdots & \vdots \\ \Delta m_{\eta 1} & \Delta m_{\eta 3} & \cdots & 0 & \cdots & \Delta m_{\eta\eta} \end{bmatrix}_{\frac{\eta+1}{2}\times\frac{\eta+1}{2}},\ q_s=\begin{bmatrix} q_1 \\ q_3 \\ \vdots \\ q_\eta \end{bmatrix}_{1\times\frac{\eta+1}{2}},$$

$$p_s=\begin{bmatrix} \Delta k_{1\,i}-\lambda_i\Delta m_{1\,i} \\ \Delta k_{3\,i}-\lambda_i\Delta m_{3\,i} \\ \vdots \\ \Delta k_{\eta\,i}-\lambda_i\Delta m_{\eta\,i} \end{bmatrix}_{\frac{\eta+1}{2}\times 1}.\ \text{where } i=1,3,5,\cdots.$$

The definition of different matrices used in Eq. (33) to solve the even-order modal parameters of the non-uniform beam is as

$$A_s = \begin{bmatrix} m_2(\lambda_i - \lambda_2) & & & 0 \\ & m_4(\lambda_i - \lambda_4) & & \\ & & \ddots & \\ 0 & & & m_\eta(\lambda_i - \lambda_\eta) \end{bmatrix}_{\frac{\eta}{2}\times\frac{\eta}{2}}, B_s = \begin{bmatrix} \Delta k_{22} & \cdots & \Delta k_{2\,i-2} & 0 & \Delta k_{2\,i+2} & \cdots & \Delta k_{2\eta} \\ \Delta k_{42} & \cdots & \Delta k_{4\,i-2} & 0 & \Delta k_{4\,i+2} & \cdots & \Delta k_{4\eta} \\ \vdots & \vdots & \vdots & \vdots & \vdots & \vdots & \vdots \\ \vdots & \vdots & \vdots & \vdots & \vdots & \vdots & \vdots \\ \Delta k_{\eta 2} & \cdots & \Delta k_{\eta\,i-2} & 0 & \Delta k_{\eta\,i+2} & \cdots & \Delta k_{\eta\eta} \end{bmatrix}_{\frac{\eta}{2}\times\frac{\eta}{2}}, q_s = \begin{bmatrix} q_2 \\ q_4 \\ \vdots \\ q_\eta \end{bmatrix}_{1\times\frac{\eta}{2}}$$

$$C_s = \begin{bmatrix} \Delta m_{22} & \Delta m_{24} & \cdots & \Delta m_{2\eta} \\ \Delta m_{42} & \Delta m_{44} & \cdots & \Delta m_{4\eta} \\ \vdots & \vdots & \vdots & \vdots \\ \Delta m_{\eta 2} & \Delta m_{\eta 4} & \cdots & \Delta m_{\eta\eta} \end{bmatrix}_{\frac{\eta}{2}\times\frac{\eta}{2}}, D_s = \begin{bmatrix} m_2 + \Delta m_{22} & \Delta m_{24} & \cdots & 0 & \cdots & \Delta m_{2\eta} \\ \Delta m_{42} & m_4 + \Delta m_{44} & \cdots & 0 & \cdots & \Delta m_{4\eta} \\ \vdots & \vdots & \vdots & \vdots & \vdots & \vdots \\ \Delta m_{i2} & \Delta m_{i4} & \cdots & 0 & \cdots & \Delta m_{i\eta} \\ \vdots & \vdots & \vdots & \vdots & \vdots & \vdots \\ \Delta m_{\eta 2} & \Delta m_{\eta 4} & \cdots & 0 & \cdots & \Delta m_{\eta\eta} \end{bmatrix}_{\frac{\eta}{2}\times\frac{\eta}{2}}, p_s = \begin{bmatrix} \Delta k_{2\,i} - \lambda_i \Delta m_{2\,i} \\ \Delta k_{4\,i} - \lambda_i \Delta m_{4\,i} \\ \vdots \\ \Delta k_{\eta\,i} - \lambda_i \Delta m_{\eta\,i} \end{bmatrix}_{\frac{\eta}{2}\times 1}.$$

where i=2, 4, 6, $\cdots$.

Appendix C

The model of the uniform beam with complete elastic supports is shown in Fig. 1(d). Eq. (9) can be solved using the transfer matrix method. The i^{th} span modal function of the uniform beam with complete elastic supports can be written as

$$Y_i(x) = A_i\, sin(ax) + B_i\, cos(ax) + C_i\, sinh(ax) + D_i\, cosh(ax) \tag{c.1}$$

where $a^4 = m\omega^2/EI$, ω is the circular frequency, A_i, B_i, C_i and D_i are the constants of the i^{th} span. According to the deformation compatibility condition in each elastic support, we can get

In the first elastic support

$$\left.\begin{aligned} Y_1''(0) &= 0 \\ k_1 Y_1(0) &= -EIY_1'''(0) \end{aligned}\right\} \tag{c.2}$$

In the last elastic support

$$\left.\begin{aligned} Y_n''(L_n) &= 0 \\ k_{n+1} Y_n(L_n) &= EIY_n'''(L_n) \end{aligned}\right\} \tag{c.3}$$

In the 2^{nd}-n^{th} elastic support

$$\left.\begin{aligned} Y_{i-1}(L_{i-1}) &= Y_i(0) \\ Y_{i-1}'(L_{i-1}) &= Y_i'(0) \\ Y_{i-1}''(L_{i-1}) &= Y_i''(0) \\ EIY_{i-1}'''(L_{i-1}) &= EIY_i'''(0) + k_i Y_i(0) \end{aligned}\right\} \tag{c.4}$$

Substitution of Eq. (c.1) into Eq. (c.4) yields

$$\begin{bmatrix} A_i & B_i & C_i & D_i \end{bmatrix}^T = \boldsymbol{U_i H_{i-1}} \begin{bmatrix} A_{i-1} & B_{i-1} & C_{i-1} & D_{i-1} \end{bmatrix}^T \tag{c.5}$$

where $\boldsymbol{U_i}=\begin{bmatrix} \frac{k_i}{2a^3EI} & \frac{1}{2} & 0 & \frac{1}{2} \\ \frac{1}{2} & 0 & \frac{1}{2} & 0 \\ \frac{-k_i}{2a^3EI} & \frac{1}{2} & 0 & -\frac{1}{2} \\ \frac{1}{2} & 0 & -\frac{1}{2} & 0 \end{bmatrix}$, $\boldsymbol{H_{i-1}}=\begin{bmatrix} sin(aL_{i-1}) & cos(aL_{i-1}) & sinh(aL_{i-1}) & cosh(aL_{i-1}) \\ cos(aL_{i-1}) & -sin(aL_{i-1}) & cosh(aL_{i-1}) & sinh(aL_{i-1}) \\ sin(aL_{i-1}) & cos(aL_{i-1}) & -sinh(aL_{i-1}) & -cosh(aL_{i-1}) \\ cos(aL_{i-1}) & -sin(aL_{i-1}) & -cosh(aL_{i-1}) & -sinh(aL_{i-1}) \end{bmatrix}$.

Recycling using the Eq. (c.5), we can get

$$\begin{bmatrix} A_n & B_n & C_n & D_n \end{bmatrix}^T = \boldsymbol{U_n N_{n-1} U_{n-1} N_{n-2}} \cdots \boldsymbol{U_2 N_1} \begin{bmatrix} A_1 & B_1 & C_1 & D_1 \end{bmatrix}^T \tag{c.6}$$

Substituting Eq. (c.1) into Eq. (c.2) and Eq. (c.3), we have

$$\boldsymbol{\Phi}\begin{bmatrix} A_n & B_n & C_n & D_n \end{bmatrix}^T = \mathbf{0} \tag{c.7}$$

$$\begin{bmatrix} A_1 & B_1 & C_1 & D_1 \end{bmatrix}^T = \boldsymbol{\Psi}\begin{bmatrix} B_1 & C_1 \end{bmatrix}^T \tag{c.8}$$

where $\boldsymbol{\Psi}=\begin{bmatrix} \frac{2k_1}{a^3EI} & 1 & 0 & 1 \\ 1 & 0 & 1 & 0 \end{bmatrix}^T$,

$$\boldsymbol{\Phi}=\begin{bmatrix} sin(aL_n) & cos(aL_n) & -sinh(aL_n) & -cosh(aL_n) \\ \frac{k_{n+1}}{a^3EI}sin(aL_n)+cos(aL_n) & \frac{k_{n+1}}{a^3EI}cos(aL_n)-sin(aL_n) & \frac{k_{n+1}}{a^3EI}sinh(aL_n)-cosh(aL_n) & \frac{k_{n+1}}{a^3EI}cosh(aL_n)-sinh(aL_n) \end{bmatrix}$$

Substituting Eq. (c.7) and Eq. (c.8) into Eq. (c.6), we can obtain the frequency Eq. (c.9) of the uniform beam with complete elastic supports.

$$det(\boldsymbol{\Phi U_n N_{n-1} U_{n-1} N_{n-2}} \cdots \boldsymbol{U_2 N_1 \Psi})=0 \tag{c.9}$$

Using Eq. (c.9), we can get the natural frequencies of the n spans uniform beam with complete elastic supports. Substituting natural frequencies into Eq. (30) and recycling using the Eq. (c.5), we can obtain the constant values A_i, B_i, C_i and D_i. Substitution of constant values A_i, B_i, C_i and D_i into Eq. (c.1), we can get the vibration model function of the uniform beam with complete elastic supports. The dynamic characteristics of non-uniform beam with added masses and elastic supports can be obtained by this paper method using the natural frequencies and the vibration model function of the uniform beam with complete elastic supports.